Electronic Supplementary Material (ESI) for Journal of Materials Chemistry B.

Supplementary Information

Revealing the dynamic mechanism of cell-penetrating peptides across cell membrane at single-molecule level

Yuhang Zhai[a], Siying Li[a], Hui Wang[a], Yuping Shan[a,] *

[a]School of Chemistry and Life Science, Advanced Institute of Materials Science, Changchun University of Technology, Changchun 130012, China.

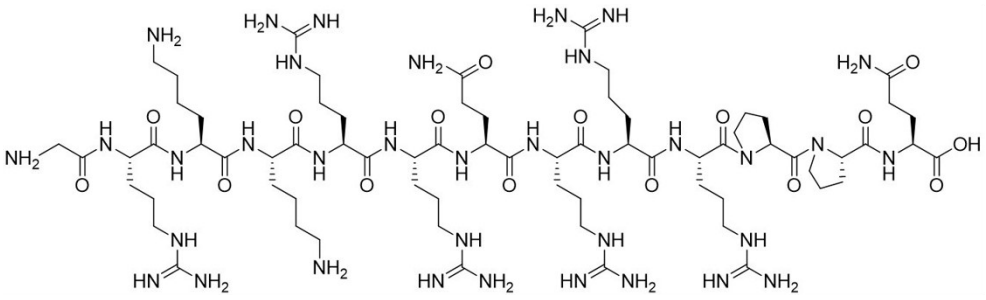

Fig. S1 The chemical structure of $TAT_{48\text{-}60}$.

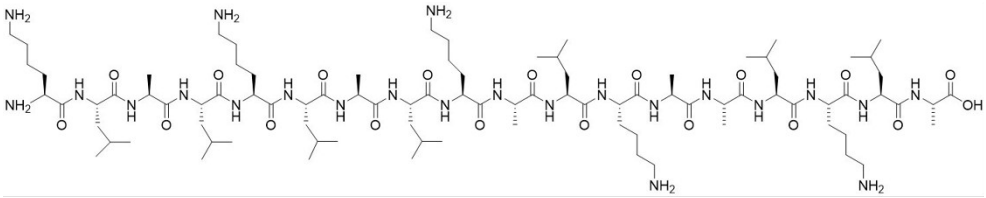

Fig. S2 The chemical structure of MAP.

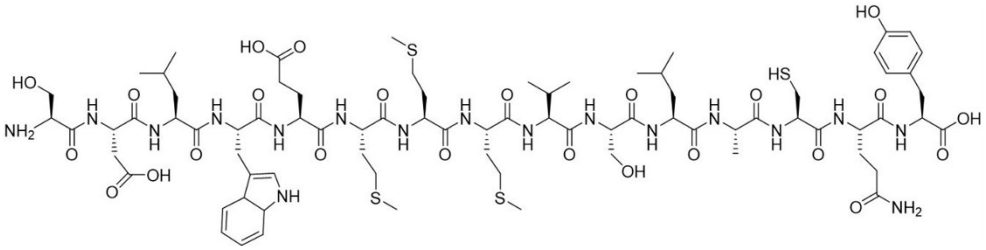

Fig. S3 The chemical structure of Pep-7.

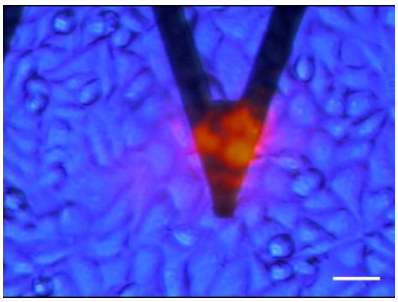

Fig. S4 The optical image of the AFM tip cantilever locating above the living HeLa cell. (Scale bar: 60 μm).

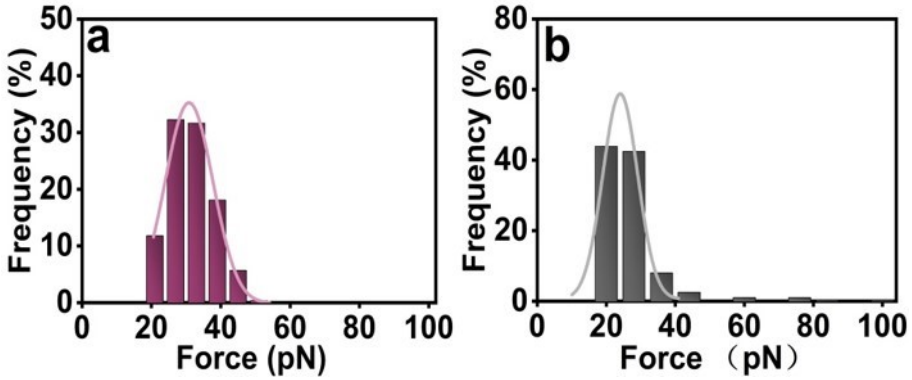

Fig. S5 The unbinding forces for TAT_{48-60} interacting with cell membrane after blocking. (a) The force distribution after blocking with free TAT_{48-60}. (b) The force distribution after blocking with free heparin. N≈500.

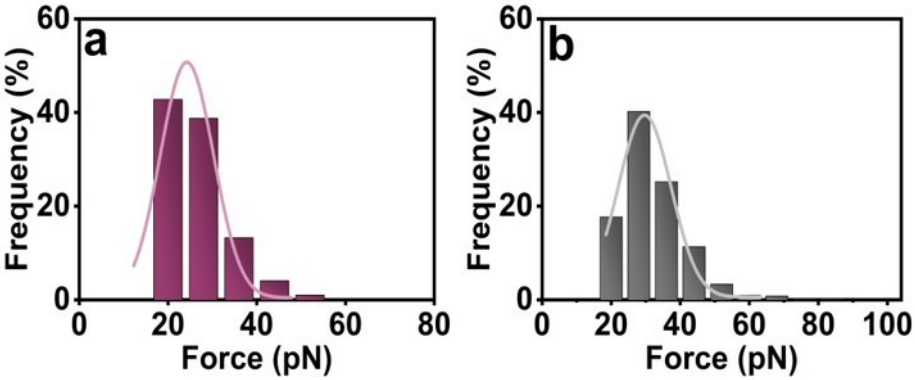

Fig. S6 The distribution histogram of unbinding forces for MAP interacting with the membrane after blocking. (a) The force distribution after blocking with free MAP. (b) The force distribution after blocking with free heparin. N≈500.

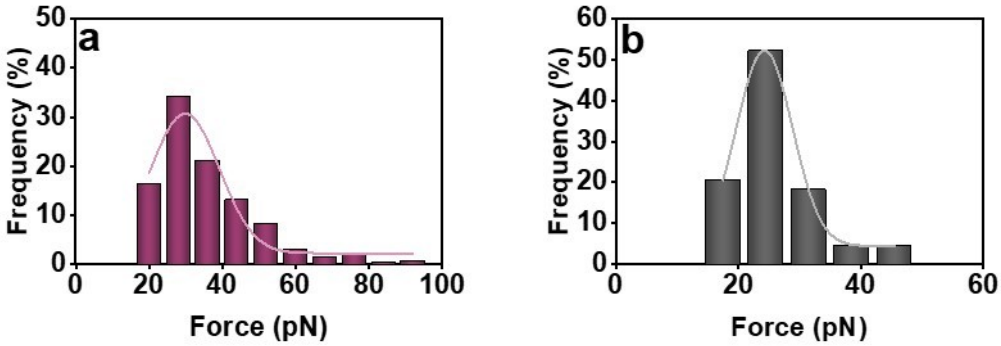

Fig. S7 The distribution histogram of unbinding forces for Pep-7 interacting with the membrane after blocking. (a) The force distribution after blocking with free Pep-7. (b) The force distribution after blocking with free heparin. N≈500.

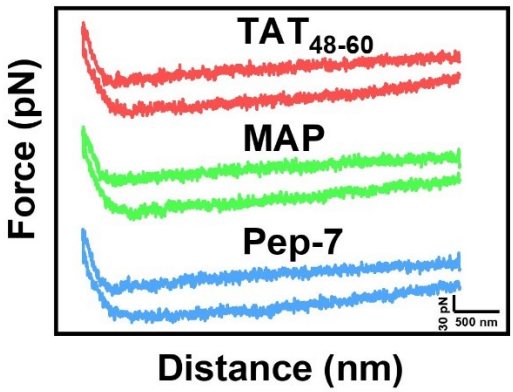

Fig. S8 The typical force-distance curves after blocking with free heparin.

Table. S1 The kinetic parameters characterizing the interaction between CPPs and the cell membrane

CPPs	τ (s)	K_{on} ($M^{-1}S^{-1}$)	K_{off} (S^{-1})	K_a (M^{-1})	K_d (M)	X_β (nm)	$\triangle G_{\beta,0}$ (K_BT)
TAT_{48-60}	0.45	1.05	1.84×10^{-3}	5.7×10^{2}	1.75×10^{-3}	0.49	27.02
MAP	0.49	1.9	3.94×10^{-3}	4.82×10^{2}	2.07×10^{-3}	0.52	26.26
Pep-7	0.94	0.7	6.74×10^{-3}	1.03×10^{2}	9.63×10^{-3}	0.64	25.77

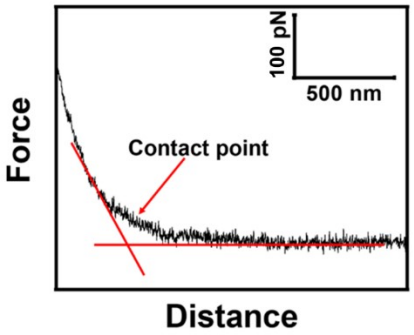

Fig. S9 The contact point between the CPPs modified AFM tip and the cell surface. The contact point is the intersection of the slope (red line) and the flat part in the force-distance curve, indicating by the red arrow.

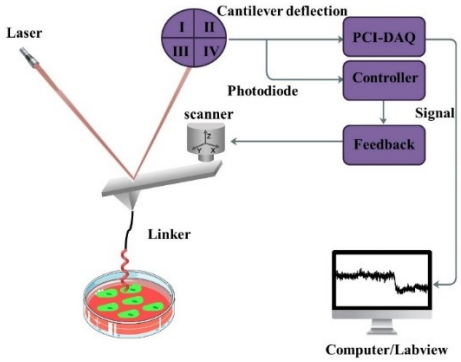

Fig. S10 Schematic diagram of the force tracing technique workflow using for detecting the cellular uptake of CPPs.

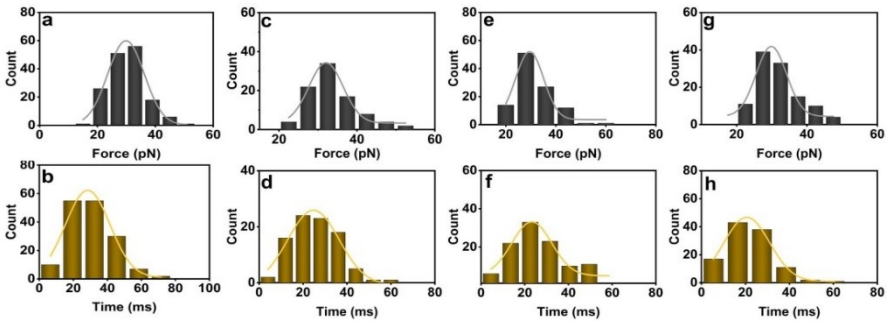

Fig. S11 The distribution histograms of force and duration for TAT_{48-60} trans-membrane after blocking. (a, c, e, g) The distribution histograms of force after blocking with free TAT_{48-60}, heparin, CPZ, and heparin + CPZ. (b, d, f, h) The distribution histograms of duration after blocking with free $TAT_{48-60,}$ heparin, CPZ, and heparin + CPZ. N≈350.

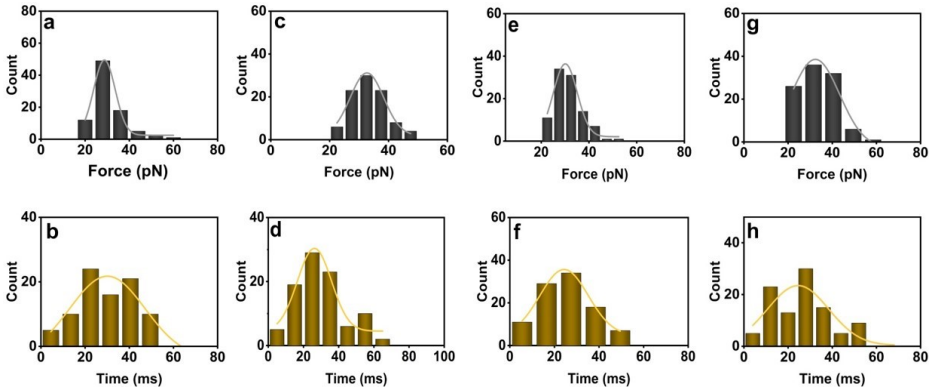

Fig. S12 The distribution histograms of force and duration for MAP trans-membrane after blocking. (a, c, e, g) The distribution histograms of force after blocking with free MAP, heparin, CPZ, and heparin + CPZ. (b, d, f, h) The distribution histograms of duration after blocking with free MAP, heparin, CPZ, and heparin + CPZ. N≈350.

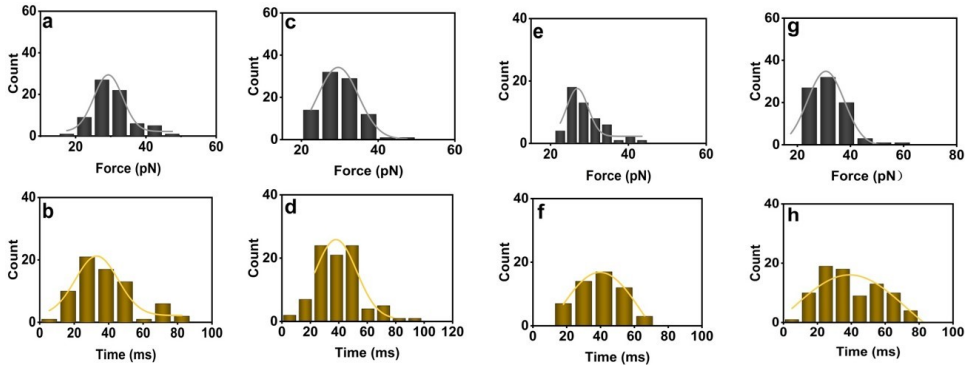

Fig. S13 The distribution histograms of force and duration for Pep-7 trans-membrane after blocking. (a, c, e, g) The distribution histograms of force after blocking with free Pep-7, heparin, CPZ, and heparin + CPZ. (b, d, f, h) The distribution histograms of duration after blocking with free Pep-7, heparin, CPZ, and heparin +CPZ. N≈350.

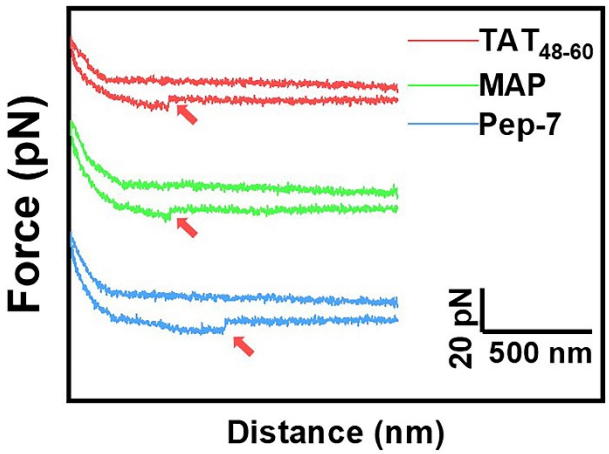

Fig. S14 The typical FD curves for CPPs interacting with Vero cells, and the red arrows indicate the force signal.

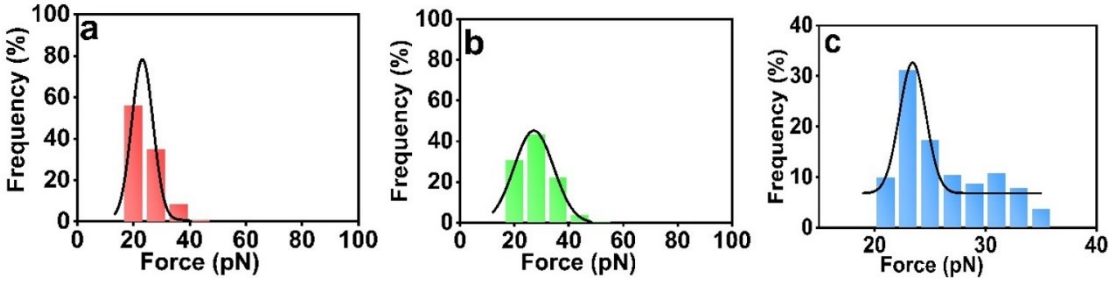

Fig. S15 The distribution histograms of unbinding force for CPPs interacting with the Vero cell membrane. (a-c) The distribution histograms of unbinding force for TAT_{48-60}, MAP, and Pep-7. N≈300.

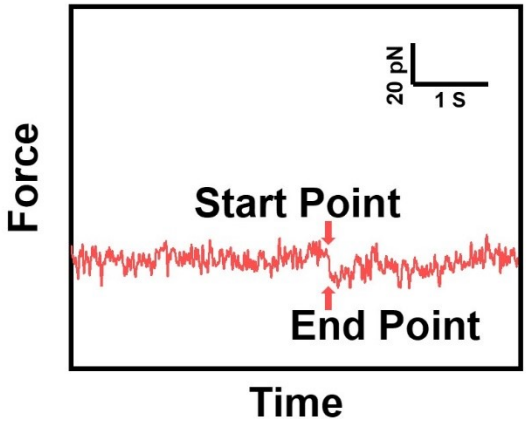

Fig. S16 The typical force-time curves of CPPs entry into Vero cells.

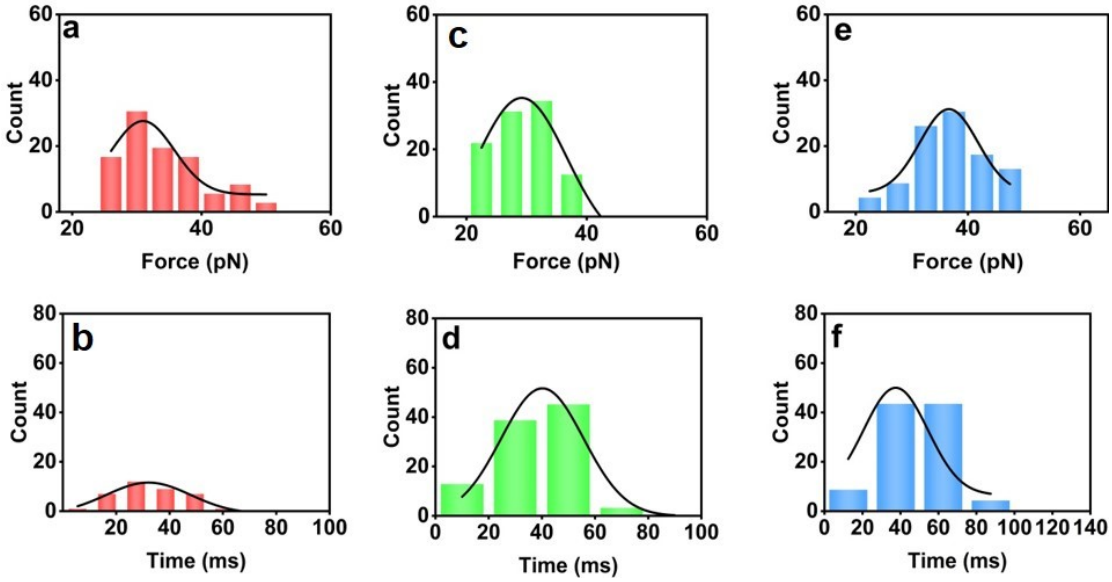

Fig. S17 The distribution histograms of force and duration for CPPs entry into Vero cells. (a, c, e) The distribution histograms of force for $TAT_{48\text{-}60}$, MAP, and Pep-7. (b, d, f) The distribution histograms of duration for $TAT_{48\text{-}60}$, MAP, and Pep-7. N≈100.

Experimental

Materials

$TAT_{48\text{-}60}$ (GRKKRRQRRRPPQ), MAP (KLALKLALKALKAALKLA) purchased from Shanghai Sangon Bioengineering Technology and Services Co. Ltd. Pep-7 (SDLWEMMMVSLACQY) was purchased from Gen Script Bioengineering Technology and Services Co. Ltd. FAM was purchased from Med Chem Express. ALexa-Fluor^{647} was purchased from Thermo Fisher Scientific. The Human cervical cancer cells (HeLa) and African green monkey kidney cells (Vero) were purchased from the Institutes of Biological Sciences (Shanghai, China).

Cell culture

HeLa cells were cultured with Dulbecco's modified Eagle's medium (DMEM,

BI), and Vero cells were cultured in minimum Eagle's medium (MEM, BI). Each type of medium was supplemented with 10% fetal bovine serum, penicillin (100 μg/mL), and streptomycin (100 μg/mL), and the cells were maintained at 37 °C in a humidified incubator containing 5% CO_2. The cells were sub-cultured for 24-36 h until 75% of the Petri dish was covered with cells. The cells were washed with PBS (phosphate buffer solution, 137 mM NaCl, 2 mM KCl, 8 mM Na_2HPO_4, 1.5 mM KH_2PO_4, pH 7.4) three times and serum-free medium once in sequence to remove cell debris and unattached cells before use. All SMFS and force tracing experiments were carried out at 37 °C.[1, 2]

Modification the AFM tips with CPPs

The CPPs were functionalized onto the AFM tip (MSCT, D-tip, Bruker, USA) as previously described.[3] In brief, the AFM tips were firstly treated with the piranha solution (H_2SO_4: 30% H_2O_2, 3:1, v/v) to clean and generate -OH on the AFM tip (Si_3N_4) surface, and then silanization by incubation with 50 μL of APTES (99 %) and 20 μL of N, N-diisopropylethylamine (99 %) for 2 h by a vapor deposition method. Subsequently, the flexible PEG linker (acetal-PEG_{45}-NHS) was attached to the silylated AFM tips using -NHS in the presence of triethylamine and trichloromethane for 2 h. Then, the PEG-modified AFM tips were immersed in an aqueous solution containing 1% citric acid for 15 min, conversion of the terminal acetal group into the aldehyde group, the amino group on peptides is covalently conjugated with the aldehyde group by immersion the AFM tip in a mixture of the peptide (0.1 mg/mL) and 4 μL of $NaCNBH_3$ for 2 h. Finally, 5 μL of 1 M ethanolamine was added to the peptide solution for 15 min to inactivate the unreacted aldehyde group.[4] After functionalization, the AFM tips were washed with PBS three times and stored in PBS at 4 ℃ until use.

SMFS measurements and dynamic force spectroscopy

All the experiments were performed with AFM 5500 (Agilent Technologies, Chandler, AZ). The experiments were carried out at 37 °C controlled by a temperature controller 325 (Agilent Technologies, Chandler, AZ). Force spectroscopy was obtained using the contact mode in serum-free culture medium (SFM) at 37 °C. The AFM tips with a normal spring constant of 0.03 N m^{-1} (MSCT, D-tip) were used, and the real spring constants of the AFM tip cantilevers were calculated with the thermal noise method in air, as previous described.[2] The dwell time was determined from the force curves, i.e., the time needed to travel from the contact point to the maximum force limit (relative maximum deflection limit of 0.2 V) and back again. The AFM tip cantilever retraction velocity can be determined by changing the scan size and sweep time.[5]

According to the single-barrier model,[2] the unbinding will occur more easily at a lower LR, and the correlation between the unbinding force and the LR is rationalized by the approximate form equation (1):

$$F_u = \frac{K_B T}{X_\beta} ln\left(\frac{r X_\beta}{K_B T K_{off}}\right) = \frac{K_B T}{X_\beta} ln\, r + \frac{K_B T}{X_\beta} ln\left(\frac{X_\beta}{K_B T K_{off}}\right), r = K_{eff} v \quad (1)$$

where F_u is the unbinding force, X_β is the transition from the bound state to the unbound state, which is separated by an energy barrier located at distance, r is the LR, K_{eff} is the effective spring constant of the AFM tip cantilever used, v is the AFM tip cantilever retraction velocity (which can be determined by changing the scan size and sweep time), K_{off} is the dissociation kinetic rate constant at zero force, K_B is the Boltzmann constant, and T is the Kelvin temperature.

The dissociation activation energy $\Delta G_{\beta,0}$ in the absence of an external force is evaluated as:[6]

$$\Delta G_{\beta,0} = - K_B T ln(\tau_D K_{off}(0)) \quad (2)$$

where τ_D denotes the diffusive relaxation time, and here $\tau_D = 10^{-9}$ S. Assuming that the bond complex can be approximated by pseudo-first-order kinetics, the K_{on} could be extracted from the BP (binding probability) measured at various contact time:[7]

$$K_{on} = \frac{\frac{1}{2} * 4\pi r_{eff}^3 N_A}{3 n_b \tau} \quad (3)$$

where r_{eff} is the effective radius of the sphere, being the sum of a sphere (7.32, 9.12, and 8.04 nm for TAT_{48-60}, MAP, and Pep-7, respectively) with the equilibrium tether (r_{eff} =3 nm for the used PEG linker)[8] and the diameter of the peptides (4.32 nm, 6.12 nm, and 5.04 nm for TAT_{48-60}, MAP, and Pep-7), n_b is the number of binding partners, and N_A is the Avogadro constant. Herein, t is set to 0.16 s, 0.32 s, 0.64 s, 0.96 s, and 1.44 s for measuring the BP. τ is the interaction time, which can be calculated from the binding probability at different dwell time by using the following equation:[9]

$$BP = A * [1 - exp(\frac{-(t - t_0)}{\tau})] \quad (4)$$

The apparent dissociation constant K_d or affinity constant K_a can also be obtained from the equations:[10]

$$K_d = K_{off}/K_{on}, \quad K_a = K_{on}/K_{off} \qquad (5)$$

Force tracing measurements and trans-membrane speed calculation

Force tracing experiments were carried out with an AFM 5500 system in a serum-free medium at 37 °C, controlled by a Model 325 temperature controller (Agilent Technologies, Chandler, AZ). The measurement of force-time curves (~4000) was obtained on at least 20 cells for each data set and collected by a 16-bit DA/AD card (PCI-6361e, National Instruments) controlled by LabVIEW (National Instruments Inc, Austin, Texas, USA). According to previous reports, the sensitivity and spring constant of the AFM tip can be detected[4]. The displacement H of CPPs entry into the cells is calculated as described in previous reports.[11] In brief, the displacement is equal to the sum of the bending distance d of the AFM tip cantilever and the stretching length h of the PEG linker:[12]

$$H = d + h \qquad (6)$$

The extended worm-like chain (WLC) model can be used to properly calculate the stretching length h of the PEG linker; the equation used for the calculation is as follows:[13]

$$\frac{FL_p}{K_BT} = \frac{1}{4}\left(1 - \frac{h}{L_0} + \frac{F}{K_0}\right)^{-2} - \frac{1}{4} + \frac{h}{L_0} - \frac{F}{K_0} \qquad (7)$$

where L_p represents the persistence length, which is 3.8 *Å*, K_B stands for the Boltzmann constant, T is the absolute temperature, L_0 is the contour length, h represents the extension length of the PEG linker, K_0 is the enthalpic correction, which is 1561±33 pN, the length of the PEG unit length is 4.2 *Å*, and the total estimated contour length L_0 for PEG is nearly 196 *Å*. The bending distance of the AFM tip cantilever can be calculated by Hooke's law as follows:[14]

$$F = k \times d \qquad (8)$$

where F is the trans-membrane force of CPPs detected from the force-time curves, and k represents the effective spring constant of the AFM tip cantilever. Therefore, the displacement H could be obtained from the above formulas (7)-(8). The duration t of CPPs entry into the cells can be obtained from the force-time signals, and the speed v could be calculated as follows:[15]

$$v = \frac{H}{t} \qquad (9)$$

Blocking experiments

Before performing single-molecule experiments, the HeLa cells were co-incubated with free CPPs (1 mg/mL), Heparin (1 μg/mL), CPZ (1 μg/mL), and Heparin (1 μg/mL) + CPZ (1 μg/mL) for 30 min, respectively. Then the cells were washed with PBS, and fresh medium was added to carry out the single-molecule experiments.

Fluorescence labeling and imaging

CPPs (200 μL, 18 μM) were reacted with excess FAM (2 μL, 26μM) for 3 h in darkness, and unreacted FAM was filtered through a Molecular Weight Cutoff (MWCO) microcon centrifugal filter device to remove. The carboxyl group on FAM and the amino group of CPP conjugates through the dehydration condensation reaction, forming amide bonds.[16] HeLa cells were sub-cultured for 24-36 h until 75% of the petri dish was covered with cells. FAM-labeled CPPs (18 μM) were co-incubated with cells in a serum-free medium for 30 min at 37 °C. The cells were washed with PBS ten times in advance of fluorescence imaging. Fluorescence imaging was performed on a fluorescence microscope (Nikon-Ti-S). FAM was excited with a 488 nm He-Ne laser. The fluorescence labeling and imaging for Vero cells are the same as those for HeLa cells. The fluorescence intensity is calculated using Image J software.

Cell imaging by confocal laser scanning microscope (CLSM)

FAM-labeled CPPs (18 μM) were incubated with the cells at 37 °C for 20 min. After washing with PBS, the cells were fixed with 4% paraformaldehyde (PFA) and washed 3 times with PBS. Then, the cells were stained with the membrane dye ALexa-Fluor^{647} for 10 min at room temperature, and washed with PBS for 10 min (three times). Finally, the cells were mounted with an imaging buffer anti-fading reagent. Fluorescence imaging was performed on a Spinning-disk confocal microscopy (SDCM). 488 nm and 640 nm lasers were used to acquire two-color images. The fluorescence number is calculated using Image J software.

References

1. M. Studenovsky, R. Pola, M. Pechar, T. Etrych, K. Ulbrich, L. Kovar, M. Kabesova and B. Rihova, *Macromol. Biosci.*, 2012, **12**, 1714-1720.
2. W. Zhao, M. Cai, H. Xu, J. Jiang and H. Wang, *Nanoscale*, 2013, **5**, 3226-3229.
3. R. Wang, S. Li, J. Li, Y. Liu, Y. Fu, J. Zhou, G. Yang, and Y. Shan, *Mol. Pharm.*, 2021, **18**, 1480-1485.
4. Q. Zhang. Y. Wang, F. Tian, H. Wang, Y. Wang, X. Ma, Q. Huang, M. Cai, Y. Ji, X. Wu, Y. Gan, Y. Yan, A. Dawson, S. Guo, J. Zhang, X. Shi, Y. Shan and X Liang, *ACS Nano*, 2022, **16**, 4059-4071.

5. B. Yang, H. Xu, S. Wang, M. Cai, Y. Shi, G. Yang, H. Wang and Y. Shan, *Nanoscale*, 2016, **8**, 18027-18031.
6. J. Zhao, S. Li, X. Pang and Y. Shan, *Chem. Commun.*, 2022, **58**, 2726-2729
7. J. Camacho, S. Bhatia, V. Reiter, D. Lauster, S. Liese, J. Rabe, A. Herrmann and R. Haag, *J. of the Amer. Chem. Soci.*, 2020, **142**, 12181-12192.
8. F. Rankla, L. Wildlinga, J. Wrussc, J. Grubera, D. Blaasc and P. Hinterdorfer, *Proc. Natl. Acad.*, 2008, **105**, 17778-17783.
9. J. Yang, S. Petitjean, M. Koehler, Q. Zhang, A. Dumitru, W. Chen, S. Derclaye, S. Vincent, P. Soumillion and D. Alsteens, *Nat. Commun.*, 2020, **11**, 4541.
10. S. Li, X. Pang, J. Zhao, Q. Zhang and Y. Shan, *Nanoscale*, 2021, **13**, 17318-17324.
11. J. Richard, K. Melikov, E. Vives, C. Ramos, B. Verbeure, M. Gait, L. Chernomordik and B. Lebleu, *J Biol. Chem.*, 2003, **278**, 585-590.
12. X. Pang, Q. Zhang, S. Li, J. Zhao, M. Cai, H. Wang, H. Xu, G. Yang and Y. Shan, *Nanoscale*, 2022, **14**, 8919-8928.
13. Y. Pan, Y. Zhang, Q. Zhang, S. Huang, B. Wang, B. Xu, Y. Shan, W. Xiong, G. Li and H. Wang, *Nanoscale Horiz*, 2018, **3**, 517-524.
14. D. Lu, X. Yang, Q. Zhang, R. Wang, S. Zhou, G. Yang and Y. Shan, *Biomater. Sci. Eng.*, 2019, **5**, 432-437.
15. M. Shan, H. Wang, S. Li, X. Zhang, G. Yang and Y. Shan, *Mol. Pharm.*, 2023, **20**, 3234-3240.
16. Y. Sakae, C. Maruyama, Y. Hamano and H. Nagatani, *Electro. Acta.*, 2023, **462**, 142769.